A model-based tracking control scheme for nonlinear industrial processes involving joint unscented Kalman filter.

BHADRA, S., PANDA, A., BHOWMICK, P. and KANNAN, S.

2023

A model-based tracking control scheme for nonlinear industrial processes involving joint unscented Kalman filter

Sanjay Bhadra[a,b], Atanu Panda[c], Parijat Bhowmick[d] and Somasundar Kannan[e]

[a]Department of Electrical Engineering, University of Engineering and Management Kolkata (UEMK), New Town, Kolkata, West Bengal, India; [b]Department of Electrical Engineering, Maulana Abul Kalam Azad University of Technology, Haringhata, Nadia, West Bengal, India;

[c]Department of Electronics and Communication Engineering, Institute of Engineering and Management (IEM), Kolkata, West Bengal, India; [d]Department of Electronics and Electrical Engineering, IIT Guwahati, Guwahati, Assam, India; [e]Department of Electrical Engineering, Robert Gordon University, Aberdeen, Scotland, UK

ABSTRACT

This paper proposes a model-based reference tracking scheme for stable, MIMO, nonlinear pro-cesses. A Joint Unscented Kalman Filtering technique is exploited here to develop a stochastic model of the physical process via simultaneous estimation of the process states and the time-varying/uncertain parameters. Unlike the existing nonlinear model predictive controllers, the proposed scheme does not involve any dynamic optimisation process, which helps to reduce the overall complexity, computation overburden and execution time. Furthermore, the proposed methodology offers robustness to process model-mismatch and considers the effects of stochas-tic disturbances. A nonlinear two-tank liquid-level control problem and a nonlinear coupled level-temperature control process are studied to demonstrate the usefulness of the proposed scheme.

KEYWORDS

Model-based control; JUKF; nonlinear MPC; TITO coupled-tank process; level-temperature control

1. Introduction

Model-based control techniques such as Internal Model Control (IMC) (Economou et al., 1986), Model Predictive Control (MPC) (Garcia et al., 1989; Qin & Badgwell, 2003; Rawlings, 2000), Model Reference Adaptive Control (MRAC) (Henningsen & Ravn, 1992; Landau, 1974), etc., have drawn significant attention of the process control engineers over the last four decades. Among these techniques, MPC has already established its worth as a popular industrial control scheme due to its ability to maintain satisfactory performance and stability for complex nonlinear processes/plants by easily adapting to new operating conditions. At its inception and throughout the 1980s, MPC was a kind of model-based control and was a variant of IMC family of controllers (Economou et al., 1986). MPC can be primarily categorised as linear MPC (Morari & Lee, 1999) and Nonlinear MPC (or NMPC) (Allgower et al., 2004) depending on the type of the underlying plant model. One of the significant challenges in designing any model-based control scheme is to select an appropriate model and to identify the process parameters. But real-time parameter identification is prone to be erroneous for higher-order and complex nonlinear industrial processes and especially when the process is subjected to stochastic uncertainties (e.g. process noise, measurement noises, random variation in process parameters). Because of these issues, both performance and stability deteriorate during real-time implementation since all industrial processes are more or less affected by the stochastic factors. Stochastic MPC (or SMPC) (Heirung et al., 2018) has drawn profound attention of the process control community over the past two decades due to its advantages over the deterministic model-based control techniques in ensuring satisfactory, safe and reli-able operation in the presence of stochastic uncertainties. In an SMPC scheme, KF/EKF/DEKF/UKF estimation technique (Haykin, 2001; Mayne, Rawlings, Rao, & Scokaert, 2000) is exploited to construct the model states taking into account the effects of stochastic uncertainties and therefore, offers better closed-loop tracking performance despite the presence of noise and random exogenous disturbance (Heirung et al., 2018; Hu, Gao, Zhong, Gao, & Subic, 2015). Other critical aspects that we need to consider for implementing an NMPC/SMPC scheme are the computational complexity and the processing time. Notably, in case of SMPC implementation (Heirung et al., 2018), both an estimation algorithm and a batch of dynamic optimisation programmes concurrently run, which causes excessive computational burden and also renders the process too much time-consuming. As a result, a significant

delay occurs in generating the required control action, which may degrade both performance and stability of the overall scheme. Apart from state estimation, often parameter estimation also becomes necessary, especially when the parameters are uncertain or keep on varying. For example, in Walker (2006), KF has been used for parameter estimation involving state constraints. Note, KF and UKF are used for linear plant models; while EKF being an extended version of KF is applied for nonlinear systems (Haykin, 2001). Apart from that, Joint EKF (JEKF) and Dual EKF (DEKF) are used for joint or sequential estimation of both states and parameters (Haykin, 2001). For recent of applications MPC, SMPC and other model-based control techniques, the articles Ma, Matusko, and Borrelli (2015), Bhadra, Panda, Bhowmick, Goswami, and Panda (2019), Wang, Chen, Ren, and Zhao (2018), Yuan, Dai, Wei, and Ming (2020), Soumya Ranjan, Bidyadhar, and Subhojit (2017), Velarde, Maestre Ishii, and Negenborn (2018), Ringbeck, Garbade, and Sauer (2020), Liu and Guo (2021), Guo and Zhao (2022), Guo and Liu (2022), and Gao et al. (2020) can be referred.

Drawn by the issues mentioned above, in this paper, we seek to develop an 'SMPC-like' nonlinear model-based control (NMBC) scheme for stable MIMO non-linear industrial processes, which utilises a JUKF estimation algorithm to construct the model states. Unlike an NMPC/SMPC, the proposed NMBC scheme does not apply any dynamic optimisation technique, instead generates the 'predicted' component of the control input by algebraically solving the steady-state response of the process model. As a result, it can significant amount of processing time. Also note that, in this paper, JUKF estimation technique has been used instead of JEKF to avoid the limitations associated with the family of EKF estimation techniques.

1.1. Notation

Notation and acronyms are standard throughout. $A \succ (\geq) 0$ indicates $A \in \mathbb{R}^{n\times n}$ is a positive defnite (semidefinite) matrix. sgn represents the signum function and is defined as: $\text{sgn}(x) = 1$ when $x \geq 0$ and $\text{sgn}(x) = -1$ when $x < 0$. The symbol $|\cdot|$ denotes the absolute value. $\hat{x}(k+l|k)$ represents the predicted value of the estimated states $\hat{x}$ at time $k+l$ based on information available at time k. $\hat{y}(k+l|k)$ denotes the predicted value of the model output y at time $k+l$ based on information available at time k. $E[\cdot]$ represents the expectation operator. $E_k[\cdot]$ gives the expected value of a random variable (vector/matrix) based on the information available at time k. The symbol $\mathcal{C}^1$ denotes the set of continuously differentiable functions. *NSR* stands for the noise-to-signal ratio.

2. Technical background and problem formulation

In this paper, we consider a class of finite dimensional, causal, nonlinear, well-defined, continuous-time systems described as

$$\dot{x} = f(x,u,d) + Gw, \quad x_0 = x(t_0); \tag{1a}$$

$$y = Cx + v, \tag{1b}$$

where $x \in \mathbb{X} \subseteq \mathbb{R}^n$ denotes the state vector, $u \in \mathbb{U} \subset \mathbb{R}^m$ is the control input vector, $y \in \mathbb{R}^p$ is the output vec-tor. While $d \in \mathbb{R}^{n_d}$, $w \in \mathbb{R}^{n_w}$ and $v \in \mathbb{R}^{n_v}$ represent the external disturbance, process noise and measurement noise. The matrix $G \in \mathbb{R}^{n\times n_w}$ models the effects of w_k on the process state x. The following technical assump-tions are satisfied by the class of systems described in (1a)–(1b).

Assumption 2.1: *The vector field $f: \mathbb{R}^n \times \mathbb{R}^m \times \mathbb{R}^{n_d} \to R^n$ continuous in u and d and locally Lipschitz in x and satisfies f(0, 0, 0)=0. there exists at least one stableoperating point (x, u, d=0) such that $A := \frac{\partial f}{\partial x}|_{(\bar{x},\bar{u},\bar{d}=0)}$ is stable and the triplet (A, B.C) is controllable and observable where $B := \frac{\partial f}{\partial u}|_{(\bar{x},\bar{u},\bar{d}=0)}$.*

Assumption 2.2: *$\mathbb{U}$ is compact, $\mathbb{X}$ is connected and the origin is contained in the interior of $\mathbb{U} \times \mathbb{X}$.*

Note that x, y, u and d all are functions of time $t \geq 0$, that is, $x = x(t)$, $y = y(t)$, $u = u(t)$ and $d = d(t)$. Below, we declare several technical assumptions which need to be satisfied for the proposed NMBC schemes to work. w and v satisfy the following assumption:

Assumption 2.3: *Both w and v are zero-mean white noise with known probability distributions p_w and p_v, respectively, and $Q = E[ww^\top]$, $R = E[vv^\top]$, $E[wv^\top] = 0$ where Q and R denote respectively the covariance matrices associated with w and v.*

w_k can also be viewed as exogenous input that cap-ture the effect of model uncertainty and in that case, G can be used as a weight to represent the uncer-tainty. d either appears as a low-frequency output disturbance or it can be introduced by perturbing some of the critical process parameters. When the disturbances and noises are considered to be random variables, (1a)–(1b) becomes a stochastic model of the process dynamics. Note that this notion is different from a system (or process) that is inherently stochastic in the sense that the system naturally exhibits random behaviour.

2.1. JUKF algorithm

This subsection presents a slightly modified version of the J UKF algorithm based on the l iterature (Julier & Uhlmann 2004; Sarkka, 2007; Wan & van der Merwe, 2000; Yu et al., 2016). I n case of J UKF, both the system's states (x_p) and the parameters (θ) are estimated simultaneously. We will define an combined state vector $x = [x_p^\top \; \theta^\top]^\top$ Filter initialisation is done following the standard procedure (Haykin, 2001). We then choose a set of $2L+1$ sigma points $\chi(k-1|k-1, i)$

$$\chi(k|k-1,i) = \hat{\chi}(k-1|k-1,i) + \int_{(k-1)T}^{kT} f(\chi(\tau,i), u(k-1))\,\mathrm{d}\tau \quad (4)$$

$$\chi(k-1|k-1,i) = \begin{cases} \hat{x}_m(k-1|k-1) \quad \text{when } i = 0 \\ \hat{x}_m(k-1|k-1) + \left(\sqrt{(L+\lambda)P(k-1|k-1)}\right)_i \\ \quad \text{when } i \in \{1,2,\ldots,L\} \\ \hat{x}_m(k-1|k-1) - \left(\sqrt{(L+\lambda)P(k-1|k-1)}\right)_i \\ \quad \text{when } i \in \{L+1, L+2,\ldots,2L\} \end{cases} \quad (2)$$

where $\lambda = \alpha^2(L+\kappa) - L$; $\kappa \in \mathbb{R}_{\geq 0}$ is a secondary scaling factor; α is another constant determined by the distribution of the sigma points around $\hat{\chi}(k-1|k-1)$ and usually lies in the range $[10^{-4}, 1]$. Note the sigma points are symmetrically distributed about $\hat{x}(k-1|k-1)$ and they are derived based on the esti-mated states and parameters $\hat{x}_m(k-1|k-1)$ and their covariance $P(k-1|k-1)$. The weight functions are defined as

$$W^c(i) = W^m(i) = \frac{1}{2(L+\lambda)} \quad \forall\, i \in \{1,2,\ldots,2L\} \quad (3a)$$

$$W^c(0) = \frac{\lambda}{L+\lambda} + (1-\alpha^2+\beta) \quad (3b)$$

$$W^m(0) = \frac{\lambda}{L+\lambda}. \quad (3c)$$

The parameter β is used to incorporate prior knowl-edge of distribution of $x(k)$ and for the Gaussian distribution. The optimum value of β is 2. Now, the predicted values of the sigma points are obtained through the following procedure

$\forall\ i \in \{0,\ 1,\ 2,\ \ldots\ ,2L\}$. The predicted state and param-eter estimates $\hat{x}_m(k|k-1)$ are obtained from the predicted sigma points as

$$\hat{x}_m(k|k-1) = \sum_{i=0}^{2L} W^m(i)\chi(k|k-1,i). \qquad (5)$$

The error covariance matrix $P(k|k-1)$ is obtained from the predicted sigma points as:

$$P(k|k-1) = \sum_{i=0}^{2L} W^c(i)\{\chi(k|k-1,i) - \hat{x}_m(k|k-1)\} \times \{\chi(k|k-1,i) - \hat{x}_m(k|k-1)\}^\top + Q \qquad (6)$$

where Q is the process noise covariance matrix. The sigma points are now recomputed using the predicted state and parameter estimates (5) as follows:

$$\chi^*(k|k-1,i) = \begin{cases} \hat{x}_m(k|k-1) & \text{for } i = 0 \\ \hat{x}_m(k|k-1,i) + \left(\sqrt{(L+\lambda)P(k|k-1)}\right)_i & \text{where } i \in \{1,2,\ldots,L\} \\ \hat{x}_m(k|k-1,i) - \left(\sqrt{(L+\lambda)P(k|k-1)}\right)_i & \text{where } i \in \{L+1, L+2,\ldots,2L\} \end{cases} \qquad (7)$$

These sigma points $\chi^*(k|k-1,\ i)\ \forall\ i \in \{0,\ 1,\ 2,\ \ldots\ ,2L\}$ are propagated through the measured output Equation (1b) to obtain the predicted measurement as

$$\hat{y}_m(k|k-1) = \sum_{i=0}^{2L} W^m(i)\ C\chi(k|k-1,i). \qquad (8)$$

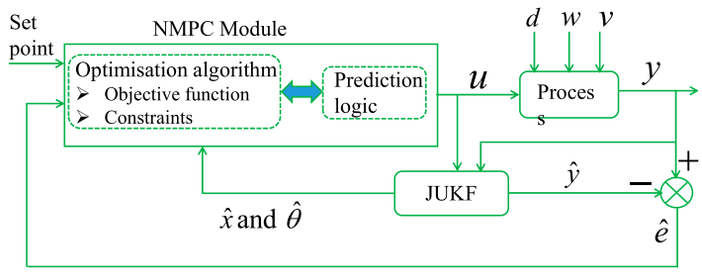

Figure 1. JUKF-based NMPC scheme.

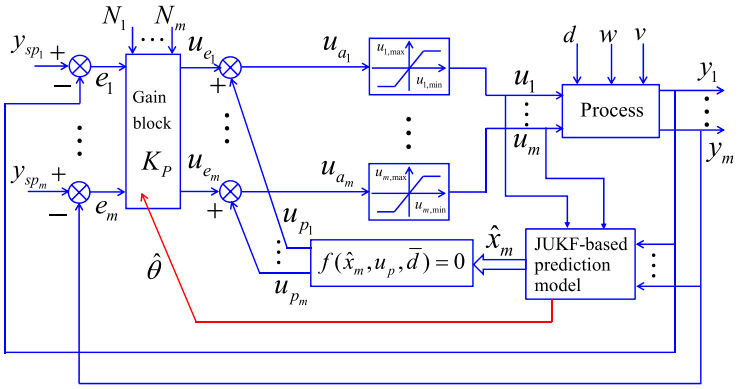

Figure 2. Schematic diagram of the JUKF-based NMBC scheme for stable nonlinear MIMO processes.

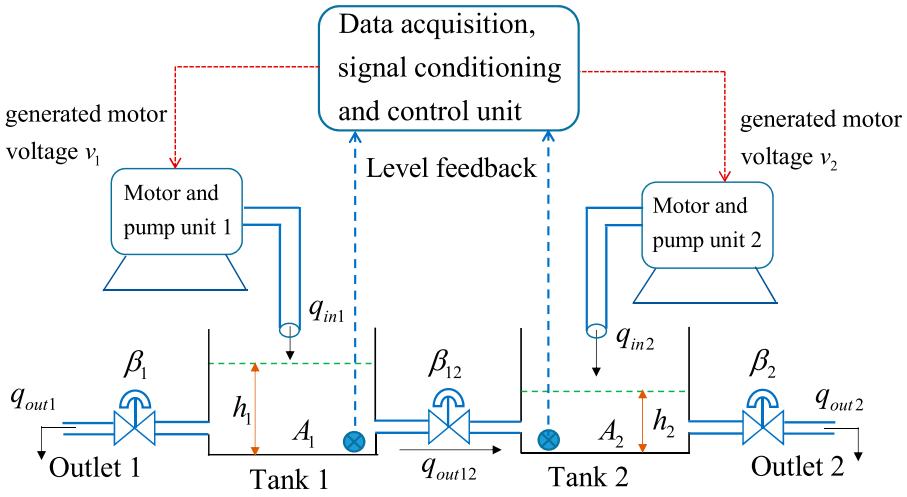

Figure 3. Schematic diagram of a two-input-two-output (TITO) coupled-tank process.

The error covariance $P_{ee}(k)$ and the cross covariance between the predicted state and parameter estimation errors $P_{\theta e}(k)$ are computed as follows:

$$P_{ee}(k) = \sum_{i=0}^{2L} W^c(i)[C\left(\chi^*(k|k-1,i)\right) - \hat{y}_m(k\,|\,k-1)] \times [C\left(\chi^*(k|k-1,i)\right) - \hat{y}_m(k|k-1)]^\top + R \tag{9}$$

$$\text{and} \quad P_{\theta e}(k) = \sum_{i=0}^{2L} W^c(i)[\chi^*(k|k-1,i) - \hat{x}_m(k|k-1)] \times [\chi^*(k|k-1,i) - \hat{x}_m(k|k-1)]^\top \tag{10}$$

where R represents the Measurement noise covariance matrix. The innovation $\gamma(k)$ is computed as

$$\gamma(k) = y(k) - \hat{y}_m(k|k-1). \tag{11}$$

Subsequently, Kalman gain matrix $K(k)$ at the k^{th} instant is defined as

$$K(k) = P_{\theta e}(k) P_{ee}(k)^{-1}. \tag{12}$$

Utilising the Kalman gain and the residual at the k^{th} instant, the state estimates $\hat{x}_m(k|k-1)$ can be updated as follows:

$$\hat{x}_m(k|k) = \hat{x}_m(k|k-1) + K(k)\gamma(k|k-1). \tag{13}$$

Similarly, the error covariance can also be updated as

$$P(k|k) = P(k|k-1) - K(k) P_{ee}(k) K(k)^{\top}. \tag{14}$$

2.2. A JUKF-based NMPC scheme

This subsection will briefly explain the working princi-ple of an SMPC scheme that utilises a JUKF algorithm to estimate the model states (x_m) and also some of the process parameters (θ). Given the desired reference trajectory $y_{sp}(k+j|k)\ \forall\ j \in \{1, 2, \ldots, N_p\}$, the JUKF-NMPC algorithm will determine the present and future values of the control signal $u(k+j|k)\ \forall\ j\{0, 1, \ldots, N_c - 1\}$ by minimising the following objective function (Figure 1)

$$\mathcal{J} = \sum_{j=1}^{N_p} W_e \left[\Delta \mathbf{e}^2(k+j|k)\right] + \sum_{j=0}^{N_c-1} W_u \left[\Delta \mathbf{u}^2(k+j|k)\right] \tag{15}$$

over $\{u(k|k), u(k+1|k), \ldots, u(k+N_c-1|k)\}$ subjected to

$$\hat{\chi}(k+j|k, i) = \begin{cases} \hat{x}_m(k+j|k) \quad \text{for } i = 0, \quad j \in \{0, 1, \ldots, N_p - 1\} \\ \hat{x}_m(k+j|k) + \left(\sqrt{(L+\lambda)P(k+j|k)}\right)_i \\ \text{where } i \in \{1, 2, \ldots, L\}, \quad j \in \{0, 1, \ldots, N_p - 1\} \\ \hat{x}_m(k+j|k) - \left(\sqrt{(L+\lambda)P(k+j|k)}\right)_i \\ \text{where } i \in \{L+1, \ldots, 2L\}, \quad j \in \{0, 1, \ldots, N_p - 1\} \end{cases} \tag{16}$$

where N_p and N_c are respectively the prediction horizon and the control horizon; W_u and W_e are the weights associated with the control input $\mathbf{u}$ and the predicted deviation of $\Delta \mathbf{e} = \mathbf{y}_{sp} - \hat{\mathbf{y}}_m$ respectively. The procedure for finding the sigma points $\chi(k+j|k, i)$, predicted states $\hat{x}_m(k+j|k, i)$, predicted error covariance $P(k+j|k, i)$ and the predicted model output $\hat{y}_m(k+j|k, i)$ are the same as described in the JUKF algorithm.

2.3. Problem formulation

Given a stable nonlinear process that can be mathematically expressed by (1a)–(1b) satisfying Assumptions 2.1–2.3 and the possible stochastic behaviour, the control problem is to design a model-based tracking scheme such that the process output can satisfactorily track the desired set-point in presence of actuator saturation.

3. Designing a JUKF-based NMBC scheme

This section presents the JUKF-based NMBC scheme shown below which is the key contribution of this paper.

We will now mention several noteworthy features of the proposed scheme.

- The NMBC scheme applies to a class of stable, MIMO, nonlinear processes that can be mathematically modelled by the Equations (1a)–(1b).
- The proposed scheme exhibits robustness to process model-mismatch due to parameter variations and stochastic uncertainties (**d**, **w**, **v**).
- The controller gains (K_p in Figure 2) can be tuned online based on the real-time input and output data, which makes the proposed scheme adaptive to changes in the operating conditions and parameter variations.
- JUKF estimation technique is used to jointly estimate the model states x_m and some of the process parameters θ that are expected to vary.
- The control law does not rely on the plant model inversion, which helps to eliminate a lot issues during practical implementation.
- In contrast to NMPC/SMPC, the NMBC scheme does not involve any dynamic optimisation process, which significantly reduces the overall complexity, computational overburden and execution time.
- The proposed scheme also considers the physical constraints of the actuators by explicitly using the saturation blocks in each of the channels, as shown in Figure 2. The scheme also mitigates the risk of 'controller windup' as it does not include any integral controllers.

The working principle of the proposed JUKF-based NMBC scheme looks similar to that of the JUKF-based NMPC scheme discussed in Subsection 2.2 However, there is a subtle difference between these two methodologies. Contrary to the SMPC scheme, the NMBC scheme resort to solving the process Equation (1a) at the steady-state condition

$$f(\hat{\mathbf{x}}_m, \mathbf{u}_p, \bar{\mathbf{d}}) = 0 \qquad (17)$$

to obtain the 'predicted' component of the input $\mathbf{u}_p = [u_{p_1}, u_{p_2}, \ldots, u_{p_m}]^\top \in \mathbb{R}^m$ where $\bar{\mathbf{d}} \in \mathbb{R}^{n_d}$ is the modelled disturbance input which incorporates the effect of exogenous disturbances. Controller gain of the i^{th} channel $K_{p_{ii}}$ (i.e. the main-diagonal elements of K_p) at each time instant is selected as the inverse of the instantaneous gain of that channel, i.e. $K_{p_{ii}} = \frac{u_{p_i}}{\hat{y}_{m_i}}$ for each $i \in \{1, 2, \ldots, m\}$ where $\hat{y}_m = C\hat{x}_m$. While the off diagonal controller gain elements $K_{p_{ij}}$, $i \neq j$, are chosen on the basis of a weighted average of the steady-state cross-coupling gains. If $\hat{y}_{m_i}(t) = 0$ at some $t \geq 0$, then $K_{p_{ii}}$ may be chosen to be the preceding non-zero gain value of that particular channel. The total control effort $\mathbf{u}_a$ is given by

$$\mathbf{u}_a(t) = NK_p(t)\mathbf{e}(t) + \mathbf{u}_p(t) \qquad (18)$$

where $N = \text{diag}\{N_1, N_2, \ldots, N_m\}$ with $N_i > 0$ represents a set of multiplying factors used online for performance improvement in a perturbed/disturbed operating condition. The upper and lower limits $u_{\max}$ and $u_{\min}$ of the saturation blocks included in the scheme (Figure 2) are decided based on the physical strength of the actuators (Skogestad & Postlethwaite, 1996). Note here that the JUKF algorithm is executed on a discrete-time basis since both in simulation and real-time implementation, all input and output data are generated or measured at discrete time steps.

4. Case study: level control of a TITO coupled-tank process

The first case study considers the liquid-level control problem of a coupled-tank system (Lian et al., 1998) (Figure 3).

4.1. Process description

Liquid-level dynamics of the coupled-tank process is described by the following differential equations:

$$\begin{cases} A_1 \dfrac{\mathrm{d}h_1}{\mathrm{d}t} = -\beta_1\sqrt{h_1} - \beta_x\sqrt{|h_1 - h_2|} \\ \quad \big[\mathrm{sgn}(h_1 - h_2)\big] + q_{in1}, \\ A_2 \dfrac{\mathrm{d}h_2}{\mathrm{d}t} = -\beta_2\sqrt{h_2} - \beta_x\sqrt{|h_1 - h_2|} \\ \quad \big[\mathrm{sgn}(h_1 - h_2)\big] + q_{in2}, \\ y_1 = h_1 \quad \text{and} \quad y_2 = h_2, \end{cases} \tag{19}$$

4.2. Simulation results

To test the tracking performance of the proposed NMBC schemes and to compare it with a NMPC scheme, the reference trajectories y_{sp_1} and y_{sp_2} were arbitrarily chosen respectively for the liquid level h_1 of Tank 1 and h_2 of Tank 2 as follow:

$$y_{sp_1} = \begin{cases} 25\,\mathrm{cm} & \forall\, t \in [0,\ 20) \\ 30\,\mathrm{cm} & \forall\, t \in [20,\ 300) \\ 27\,\mathrm{cm} & \forall\, t \in [300,\ 500] \end{cases} \quad \text{and}$$

$$y_{sp_2} = \begin{cases} 20\,\mathrm{cm} & \forall\, t \in [0,\ 20) \\ 25\,\mathrm{cm} & \forall\, t \in [20,\ 300) \\ 22\,\mathrm{cm} & \forall\, t \in [300,\ 500]. \end{cases}$$

where A_1 and A_2 indicate the respective cross-sectional areas of the tanks; h_1 and h_2 denote the respective levels of Tank 1 and Tank 2; q_{in1} and q_{in2} are the volumet-ric inflow rates of Tank 1 and Tank 2; q_{out1} and q_{out2} denote the outflow rates of the tanks; q_{out12} represent the flow rate to Tank 2 from u_1 and u_2 signify the voltages required to maintain q_{in1} and q_{in2}; $\beta_1 = a_1\sqrt{2g}$ and $\beta_2 = a_2\sqrt{2g}$ are the downstream valve coefficients of Tank 1 and Tank 2 where a_1 and a_2 denote the cross-sectional areas of the outlet pipes connected to Tank 1 and Tank 2, while $\beta_{12} = a_{12}\sqrt{2g}$ indicates the same for the value connecting the tanks where same for the valve connecting the tanks where a_{12} is the cross-sectional area of the connecting pipe. Note that h_1, h_2, u_1 and u_2 are all real-time variables defined for all $t \geq 0$ but explicit dependence of time t is omitted everywhere. Differential changes in the levels Δh_1 and Δh_2 with respect to the nominal values $\bar{h}_1$ and $\bar{h}_2$ are selected as the state variables x_1 and x_2. The process variables and their nominal values are listed in Table 1.

Table 1. Nominal values of the parameters and variables associated with the coupled-tank process.

Process variable	Nominal value
A_1 and A_2	32 cm^2
$h_{1\,\max}$ and $h_{2\,\max}$	40 cm
β_1	14.30 $\mathrm{cm}^{5/2}$/s 14.30
β_2	$\mathrm{cm}^{5/2}$/s
β_{12}	20 $\mathrm{cm}^{5/2}$/s
$u_1 = q_{in1}$	$0 \leq u_1 \leq 1000$ cm^3/s
$u_2 = q_{in2}$	$0 \leq u_2 \leq 1000$ cm^3/s
$\bar{u}_1$	114.9 cm^3/s
$\bar{u}_2$	20.95 cm^3/s
$\bar{h}_1$	25 cm
$\bar{h}_2$	20.25 cm
g	980.7 $\mathrm{cm/s}^2$

4.2.1. *Tracking response with measurement noise*

Figure 4(a,c) show the tracking response of the liquid level h_1 of Tank 1 and h_2 of Tank 2. The figures suggest that both h_1 and h_2 are closely following the respec-tive set-point trajectories y_{sp_1} and y_{sp_2} (marked by Red colour) in presence of measurement noise (NSR = 0.1). Figure 4(b,d) depict the corresponding control input demands from which it is observed that both $u_1 = q_{in,1}$ and $u_2 = q_{in,2}$ remain within the prescribed bounds. We also notice that the performance of the proposed NMBC scheme is at par with the NMPC and moreover, the control inputs sometimes exhibit more oscillations in case of NMPC than NMBC.

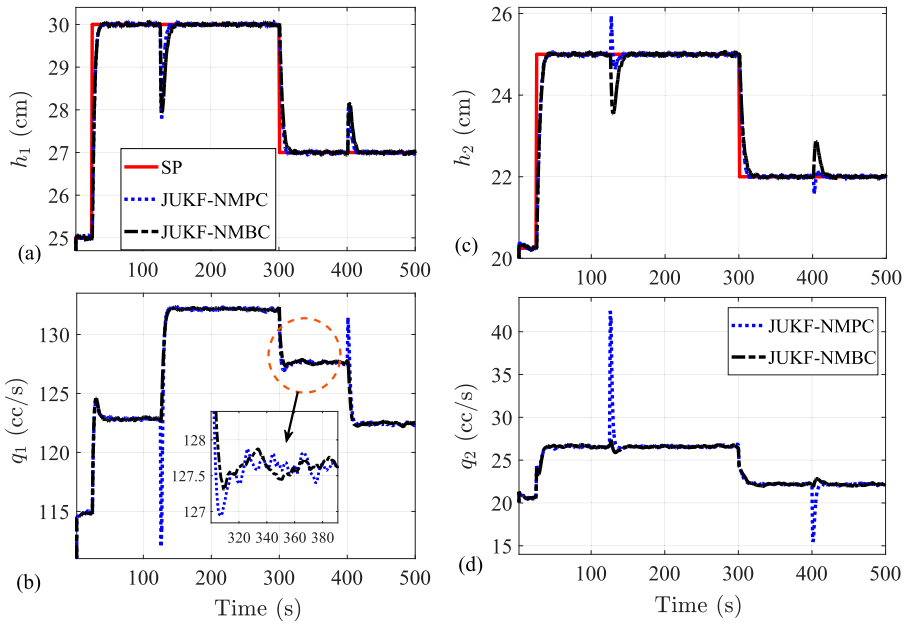

Figure 4. Tracking response of the coupled-tank process obtained via JUKF-based NMPC and NMBC schemes considering measurement noise (NSR = 0.1): (a) level h_1 of tank 1, (b) control input q_1, (c) level h_2 of tank 2, (d) control input q_2.

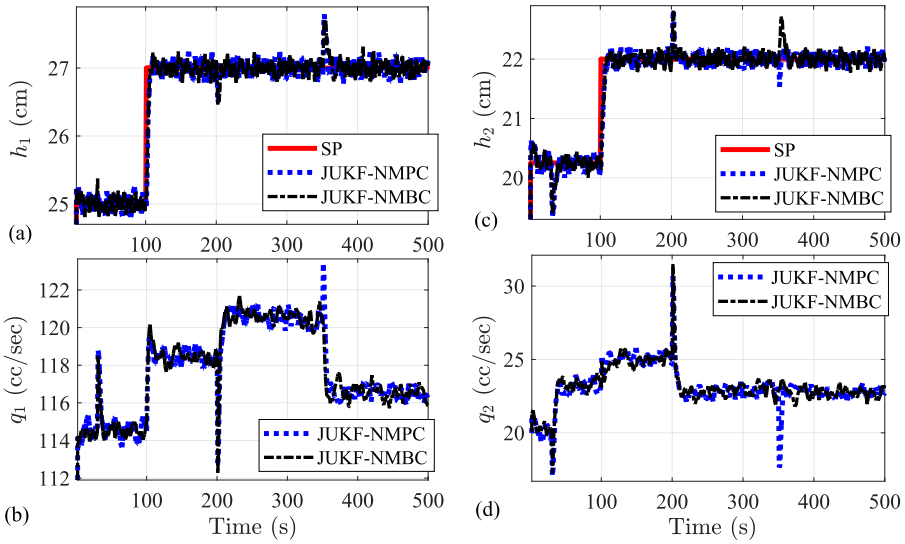

Figure 5. Set-point tracking response of the coupled-tank system obtained via applying JUKF-based NMPC and NMBC schemes considering both process model-mismatch measurement noise (NSR = 0.1): (a) level h_1 of tank 1, (b) control input q_1, (c) level h_2 of tank 2, (d) control input q_2.

4.2.2. Impact of process model-mismatch

Figure 5(a,c) shows the tracking response of the two-tank system considering the effect of both process model-mismatch and measurement noise (NSR = 0.1). The process parameters β1, β2 and β12 were perturbed as mentioned below.

$$\beta_1 = \begin{cases} 14.30 & \text{for } 0 \le t < 350\,\text{s}, \\ 13.5 & \text{for } 350\,\text{s} \le t \le 500\,\text{s}; \end{cases}$$

$$\beta_2 = \begin{cases} 14.30 & \text{for } 0 \le t < 30\,\text{s}, \\ 15.0 & \text{for } 30\,\text{s} \le t \le 500\,\text{s}; \end{cases}$$

$$\beta_{12} = \begin{cases} 20 & \text{for } 0 \le t < 200\,\text{s}, \\ 21 & \text{for } 200\,\text{s} \le t \le 500\,\text{s}; \end{cases}$$

$$T_{c0} = \begin{cases} 350 & \text{for } 0 \le t < 100, \\ 352 & \text{for } t \ge 100. \end{cases}$$

The figures suggest that despite the process model-mismatch, both of the process outputs h_1 and h_2 are satisfactorily tracking their respective set-point trajectories y_{sp_1} and y_{sp_2}. The amplitude of oscillations in the tracking responses vary within $3 - 5\%$ of the steady-state value. Figure 5(b,d) show the respective control input demands. Note here that both $q_{in,1}$ and $q_{in,2}$ remain within the specified range. The figures reveal that the performance of the NMBC scheme is compa-rable to that of the NMPC scheme.

4.3. Comparative study on the performance achieved by NMBC and NMPC schemes

This subsection will analyse the impact of varying the tuning parameter N in both NMBC and NMPC schemes for improving their dynamic performances. Figure 6 shows the tracking responses achieved by the NMBC scheme subject to four different sets of values {10, 200}, {20, 400}, {30, 600}, {40, 800} of the tuning parameters N_1 and N_2. The figure reflects that the speed of response becomes faster with increasing values of N_1 and N_2. Similarly, Figure 7 portrays the tracking response achieved by the NMPC scheme subject to $N \in \{30, 20, 10, 5\}$. The figure reveals that the speed of response improves with a decreasing value of N. Depending on the simulation responses, we conjecture that the performance of the NMBC scheme is as good as that of the NMPC scheme.

5. Case study on a coupled level and temperature control process

In this case study, we consider a benchmark two-input-two-output (TITO) level and temperature control process (Nakamoto & Watanabe, 1991) which is quite common in process and pharmaceutical industries. The salient features of this process are: highly coupled (variation in the feed flow rate affects both the liquid level and temperature of the tank) and nonlinear (square root and inverse nonlinearities are present) which renders the level and temperature control process a challenging and non-trivial task. A schematic diagram of the process is shown in Figure 8.

The process has two inputs, *viz,* feed flow rate $q_{in,1} = u_1$ and heat flow rate $q_{in,2} = u_2$; and two outputs, *viz,* liquid level $h = y_1$ and temperature $T = y_2$ of the tank. In this study, We assume that the process is adiabatic, the tank is stirred continuously throughout the experiment and the dynamics of the sensor and actuator can be neglected without loss of generality. Liquid level is measured by differential pressure level sensor while the temperature is measured by a thermocouple as indicated in Figure 8. Governing equations of the level and temperature control process are presented below:

$$\dot{x}_1 = -\frac{k}{A}x_1^{\frac{1}{2}} + \frac{1}{A}u_1, \tag{20a}$$

$$\dot{x}_2 = \frac{T_0 - x_2}{Ax_1}u_1 + \frac{1}{C_p\rho Ax_1}u_2, \tag{20b}$$

$$y_1 = x_1 \quad \text{and} \quad y_2 = x_2, \tag{20c}$$

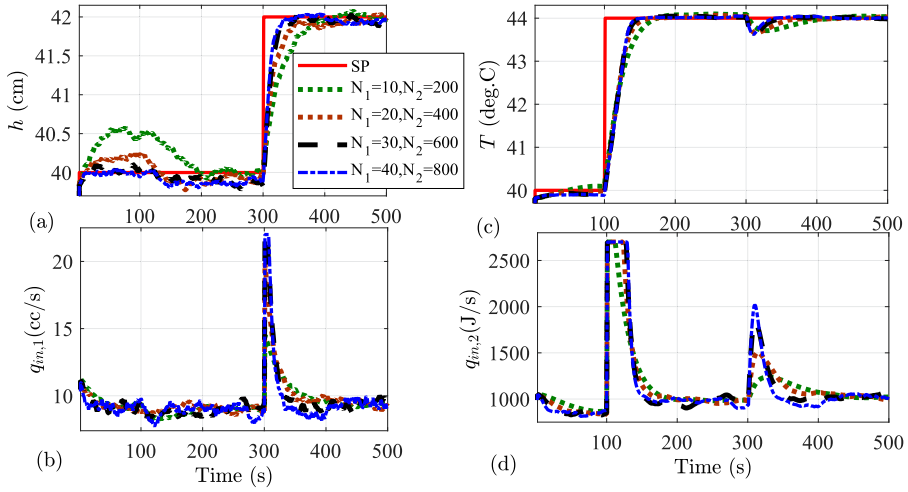

Figure 6. Set-point tracking responses of the coupled-tank process obtained via applying JUKF-based NMBC scheme subject to variation of the tuning parameters N_1 and N_2.

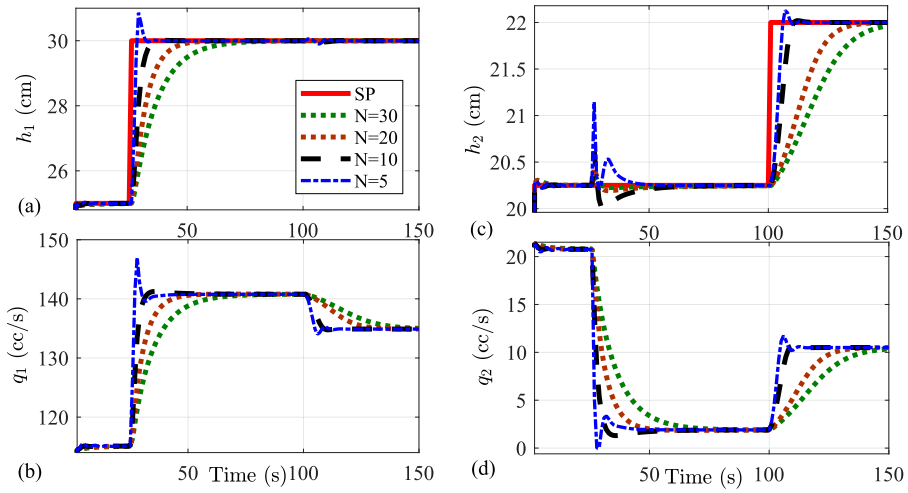

Figure 7. Set-point tracking responses of the coupled-tank process obtained via applying JUKF-based NMPC scheme subject to different values of the tuning parameter $N = 5,10,20$ and 30.

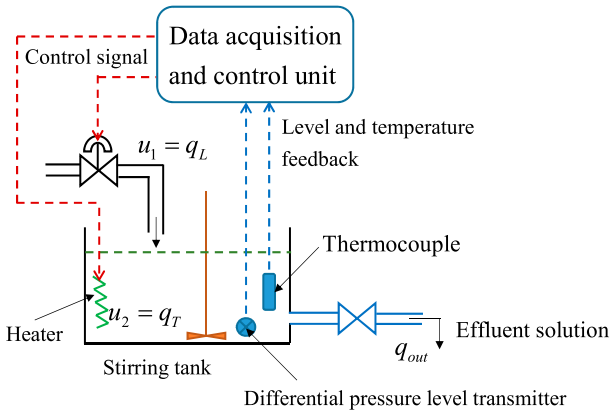

Figure 8. A benchmark level and temperature control setup.

Table 2. Nominal values of the parameters and variables associated with TITO coupled tank process.

Process variable	Nominal value
Maximum height (H)	75 cm
Diameter (D)	15.6 cm
A	191 cm^2
C_p	4.2 J g^{-1} K^{-1}
ρ	1.0 g cm^{-3}
k	1.8 $cm^{5/2}$ s^{-1}
T_0	18 °C
$u_1 = q_{in,1}$	$0 \leq u_1 \leq 22$ cm^3/s
$u_2 = q_{in,2}$	$0 \leq u_2 \leq 2700$ J/s
$\bar{x}_1$	40 cm
$\bar{x}_2$	40°C
$\bar{u}_1$	15 cm^3/s
$\bar{u}_2$	1500 J/s

where the states x1 and x2 represent the liquid level (in cm) and temperature (in $\circ$ C) of the tank. The process variables and their nominal values are listed in Table 2.

The control objective of this case study is to regulate (or track) (i) the liquid level of the tank by adjusting the control valve and (ii) the temperature of the tankby manipulating the current input to the electric heater, according to given reference (or set-point) trajectories of the level and temperature.

5.1. Simulation results

We will now analyse the Matlab simulation responses of the benchmark level and temperature control process subjected to a multi-step input applying both NMPC and NMBC techniques. The desired set-point trajectories are mentioned as following:

$$y_{sp_1} = \begin{cases} 40\,\text{cm} & \forall\, t \in [0,\ 250) \\ 44.5\,\text{cm} & \forall\, t \in [250,\ 500) \\ 40\,\text{cm} & \forall\, t \in [500,\ 1000] \end{cases} \quad \text{and}$$

$$y_{sp_2} = \begin{cases} 40^\circ C & \forall\, t \in [0,\ 250) \\ 44.5^\circ C & \forall\, t \in [250,\ 500) \\ 40^\circ C & \forall\, t \in [500,\ 1000]. \end{cases}$$

5.1.1. Tracking response with measurement noise

Figure 9(a,c) show the tracking response of the liquid level h and the temperature T of the tank. The figures suggest that the process outputs h and T are closely following the respective set-point trajectories y_{sp_1} and y_{sp_2} (marked by Red colour) in presence of measurement noise (NSR = 0.1). Figure 9(b,d) depict the corresponding control input demands from which it is observed that both $u_{in,1}$ and $u_{in,2}$ remain within the prescribed bounds. We also notice that the performance OF the proposed NMBC scheme is at par with the NMPC and moreover, the control inputs sometimes exhibit more oscillations in case of NMPC than NMPC.

5.1.2. Impact of process model-mismatch

Figure 10(a,c) shows the tracking response of the closed-loop system considering the effect of both process model-mismatch and measurement noise (NSR = 0.1). The process parameter T_0 in (20b) was perturbed to 16°C from its nominal value 18°C at $t = 20$ s. The figures suggest that despite the process model-mismatch, both of the process outputs h and T are satis-factorily tracking their respective set-point trajectories y_{sp_1} and y_{sp_2}. The amplitude of oscillations in the tracking responses vary within $3 - 5\%$ of the steady-state value. Figure 10(b,d) show the respective control input demands. Note here that both $q_{in,1}$ and $q_{in,2}$ remain within the specified range. The figures reveal that the performance of the NMBC scheme is comparable to that of the NMPC scheme.

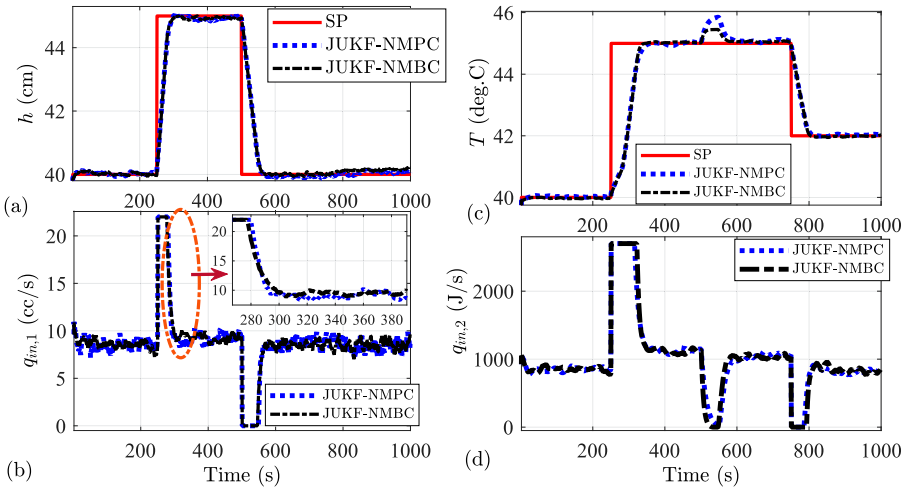

Figure 9. Set-point tracking response of the level and temperature control process obtained via JUKF-based NMPC and NMBC schemes considering measurement noise (NSR = 0.1): (a) level h, (b) control input $q_{in,1}$, (c) temperature T, (d) control input $q_{in,2}$.

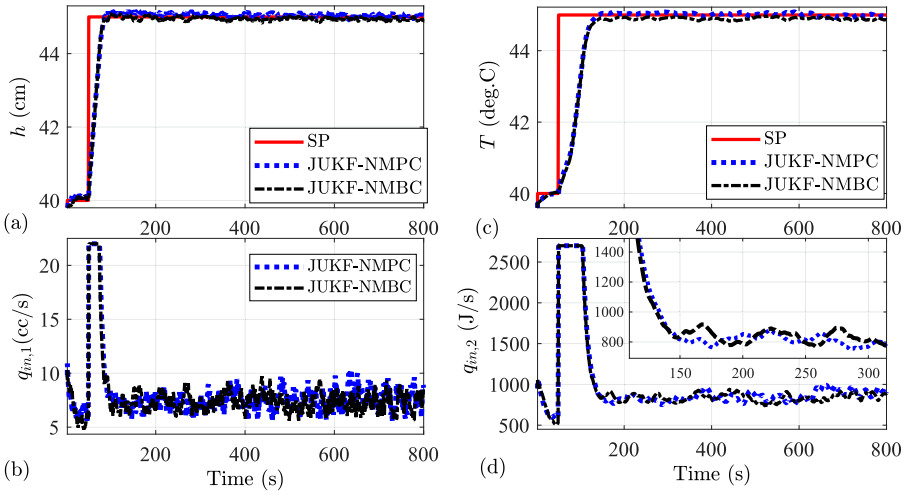

Figure 10. Set-point tracking response of the level and temperature control process obtained via JUKF-based NMPC and NMBC schemes considering both process model-mismatch and measurement noise (NSR = 0.1): (a) level h, (b) control input $q_{in,1}$, (c) temperature T, (d) control input $q_{in,2}$.

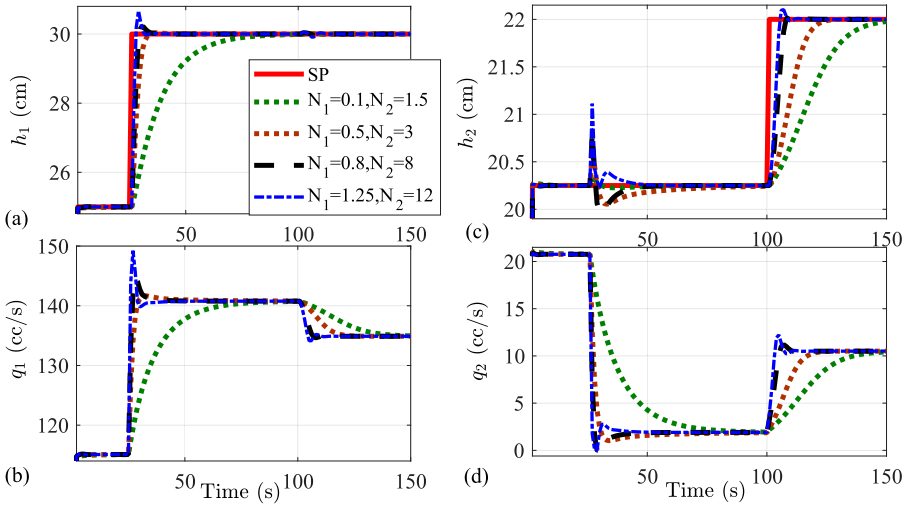

Figure 11. Tracking responses of the level and temperature control process obtained via applying JUKF-based NMBC scheme subject to variation of the tuning parameters N_1 and N_2.

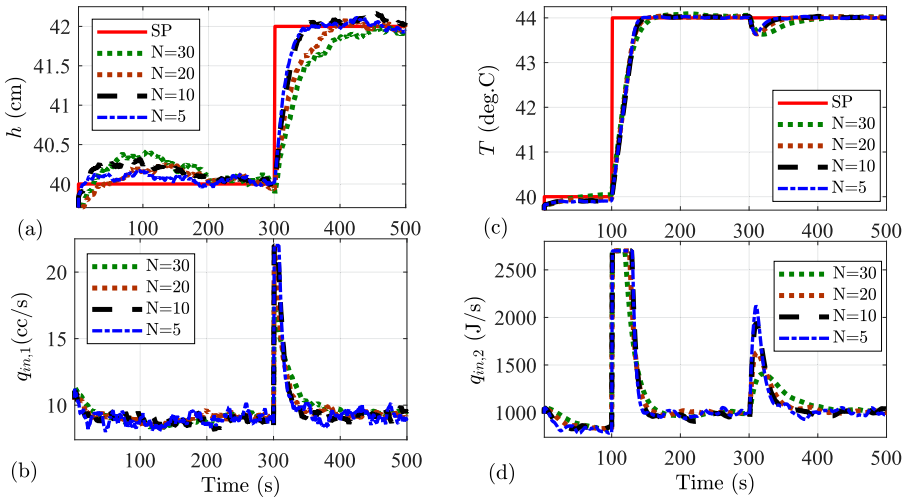

Figure 12. Tracking responses of the level and temperature control process obtained via applying JUKF-based NMPC scheme subject to different values of the tuning parameter $N = 5,10,20$ and 30.

5.1.3. Comparative study between NMPC and NMBC

This subsection will analyse the role of tuning parameter N included in both NMBC and NMPC schemes for improving the dynamic performance of the closed-loop system. Figure 11 shows the tracking responses achieved by the NMBC scheme subject to four different sets of values of the tuning parameters N_1 and N_2 given by {0.1, 1.0}, {0.5, 5}, {0.8, 8}, {1.25, 12.5}. The figure reflects that the speed of response becomes faster with increasing values of N_1 and N_2. Similarly, Figure 12 portrays the tracking response achieved by the NMPC scheme subject to $N \in \{30, 20, 10, 5\}$. The figure reveals that the speed of response improves with a decreasing value of N. Depending on the simulation responses, we conjecture that the performance of the NMBC scheme is as good as that of the NMPC scheme.

6. Conclusion

This paper put forward a nonlinear model-based tracking control (NMBC) scheme for stable stochastic industrial processes. The proposed scheme implements a JUKF estimation algorithm to jointly estimate the model states and some of the process parameters which are prone to vary. In contrast to the NMPC techniques, the NMBC scheme does not involve any dynamic optimisation method. Instead, the latter exploits a steady-state behaviour of the process model to design the 'predicted' control input. Two case studies on a two-tank process and a coupled level-temperature control process have been taken up to show the usefulness of the proposed scheme. Simulation results suggest that the NMBC scheme also offer robustness against process model-mismatch and stochastic uncertainties (e.g. process noise and measurement noise).

Acknowledgments

The authors express their sincere thanks and gratitude to the anonymous reviewers and the concerned Associate Editor for giving constructive comments and suggestions those have greatly helped to improve the quality and clarity of the paper. The authors would also like to thank Prof Alexander Lanzon, Dept. of EEE, University of Manchester, UK, for giving useful tips to polish this paper. We also confirm that the contributions of this paper are solely based on our own original research work that has not been published previously and neither is under review in any other journal.

Disclosure statement

No potential conflict of interest was reported by the author(s).

Funding

This work has been supported by the Science and Engineering Research Board (SERB), DST, India [grant number SRG/2022/000892].

References

Allgower, F., Findeisen, R., & Nagy, Z. K. (2004). Nonlinear
Nonlinear model predictive control: From theory to application. *Jour-nal of the Chinese Institute of Chemical Engineers*, *35*(3), 299–315.

Bhadra, S., Panda, A., Bhowmick, P., Goswami, S., & Panda, R. C. (2019, July). Design and application of nonlinear model-based tracking control schemes employing DEKF estima-tion. *Optimal Control Applications and Methods*, *40*(5), 938–960. https://doi.org/10.1002/oca.v40.5

Economou, C. G., Morari, M., & Palsson, B. O. (1986). Inter-nal model control: 5. Extension to nonlinear system. *Indus-trial & Engineering Chemistry Research*, *25*(2), 403–

Gao, Z., Liu, Y., Yang, C., & Chen, X. (2020). Unscented Kalman filter for continuous-time nonlinear fractional-order systems with process and measurement noises. *Asian Journal of Control*, *22*(5), 1961–1972. https://doi.org/10.1002/asjc.v22.5

Garcia, C. E., Prett, D. M., & Morari, M. (1989). Model predictive control: Theory and practice – a survey. *Automatica*, *25*(3), 335–348. https://doi.org/10.1016/0005-1098(89)90002-2

Guo, G., & Liu, J. (2022, December). A stochastic model-based fusion algorithm for enhanced localization of land vehicles. *IEEE Transactions on Instrumentation and Measurement*, *71*, 1–10.Article ID 8500810, https://doi.org/10.1109/TIM.2021.3137566

Guo, G., & Zhao, S. (2022, March). 3D multi-Object tracking with adaptive cubature Kalman filter for autonomous driving. *IEEE Transactions on Intelligent Vehicles*1–8. https://doi.org/10.1109/TIV.2022.3158419 .

Haykin, S. (2001). *Kalman filtering and neural networks* (1st ed.). Wiley & Sons, Inc..

Heirung, T. K. N., Paulson, J. A., O'Leary, J., & Mesbah, A. (2018). Stochastic model predictive control – how does it work? *Computers and Chemical Engineering*, *114*(9), 158–170. https://doi.org/10.1016/j.compchemeng.2017.10.026

Henningsen, A., & Ravn, O. (1992). Model reference adaptive control and adaptive stability augmentation. *IFAC Proceedings Volumes*, *25*(14), 209–214. https://doi.org/10.1016/S1474-6670(17)50737-5

Hu, G., Gao, S., Zhong, Y., Gao, B., & Subic, A. (2015). Modified strong tracking unscented Kalman filter for nonlinear state estimation with process model uncertainty. *International Journal of Adaptive Control and Signal Processing*, *29*(12), 1561–1577. https://doi.org/10.1002/acs.2572

Julier, S. J., & Uhlmann, J. K. (2004). Unscented filtering and nonlinear estimation. *Proceedings of the IEEE*, *92*(3), 401–422. https://doi.org/10.1109/JPROC.2003.823141

Landau, I. D. (1974). A survey of model reference adaptive techniques – theory and applications. *Automatica*, *10*(4), 353–379. https://doi.org/10.1016/0005-1098(74)90064-8

Lian, S. T., Marzuki, K., & Rubiyah, Y. (1998). Tuning of a neuro-fuzzy controller by genetic algorithms with an application to a coupled-tank liquid-level control system. *Engineering Applications of Artificial Intelligence*, *11*(4), 517–529. https://doi.org/10.1016/S0952-1976(98)00012-8

Liu, J., & Guo, G. (2021). Vehicle localization during GPS outages with extended Kalman filter and deep learning. *IEEE Transactions on Instrumentation and Measurement*, *70*, 1–10. Article ID 7503410, https://doi.org/10.1109/TIM. 2021.3097401

Ma, Y., Matusko, J., & Borrelli, F. (2015). Stochastic model predictive control for building HVAC systems: complexity and conservatism. *IEEE Transactions on Control Systems Technology*, *23*(1), 101–116. https://doi.org/10.1109/TCST. 2014.2313736

Mayne, D. Q., Rawlings, J. B., Rao, C. V., & Scokaert, P. O. M. (2000). Constrained model predictive control: Stability and optimality. *Automatica*, *36*(6), 789–814. https://doi.org/10.1016/S0005-1098(99)00214-9

Morari, M., & Lee, J. H. (1999). Model predictive control: Past, present and future. *Computers and Chemical Engineering*, *23*(4–5), 667–682. https://doi.org/10.1016/S0098-1354(98)00301-9

Nakamoto, K., & Watanabe, N. (1991). Multivariable control experiments of non-linear chemical processes using non-linear feedback transformation. *Journal of Process Con-trol*, *1*(3), 140–145. https://doi.org/10.1016/0959-1524(91) 85002-Z

Qin, S. J., & Badgwell, T. A. (2003). A survey of industrial model predictive control technology. *Control Engineering Practice*, *11*(7), 733–764. https://doi.org/10.1016/S0967-0661(02)00186-7

Rawlings, J. B. (2000). Tutorial overview of model predictive control. *IEEE Control Systems Magazine*, *20*(3), 38–52. https://doi.org/10.1109/37.845037

Ringbeck, F., Garbade, M., & Sauer, D. U. (2020). Uncertainty-aware state estimation for electrochemical model-based fast charging control of lithium-ion batteries. *Journal of Power Sources*, *470*, Article ID 228221. https://doi.org/10. 1016/j.jpowsour.2020.228221

Sarkka, S. (2007). On unscented Kalman filtering for state estimation of continuous-time nonlinear systems. *IEEE Transactions on Automatic Control*, *52*(9), 1631–1641. https://doi.org/10.1109/TAC.2007.904453

Skogestad, S., & Postlethwaite, I. (1996). *Multivariable feedback control: Analysis and design* (1st ed.). Wiley. Soumya Ranjan, M., Bidyadhar, S., & Subhojit, G. (2017). PI controller design for a coupled tank system using LMI approach: An experimental study. *Journal of Chemical Engineering & Process Technology*, *7:266*(1), 1–8.

Velarde, P., Maestre J, M., Ishii, H., & Negenborn R, R. (2018). Vulnerabilities in Lagrange-based distributed model predictive control. *Optimal Control Applications and Methods*, *39*(2), 601–621. https://doi.org/10.1002/oca.v39.2

Walker, D. M. (2006). Parameter estimation using Kalman filters with constraints. *International Journal of Bifurcation and Chaos*, *16*(4), 1067–1078. https://doi.org/10.1142/S0218127406015325

Wan, E. A., & van der Merwe, R. (2000, October). The unscented Kalman filter for nonlinear estimation. In *Proceedings of the IEEE Adaptive Systems for Signal Processing, Communications and Control Symposium* (pp. 153–158).

Wang, T., Chen, S., Ren, H., & Zhao, Y. (2018). Model-based unscented Kalman filter observer design for lithium-ion battery state of charge estimation. *International Journal of Energy Research*, *42*(4), 1603–1614. https://doi.org/10.1002/er.v42.4

Yu, A., Liu, Y., Zhu, J., & Dong, Z. (2016). An improved dual unscented Kalman filter for state and parameter estimation. *Asian Journal of Control*, *18*(4), 1427–1440. https://doi.org/10.1002/asjc.v18.4

Yuan, H., Dai, H., Wei, X., & Ming, P. (2020). Model-based observers for internal states estimation and control of proton exchange membrane fuel cell system: A review. *Journal of Power Sources*, *468*, Article ID 228376. https://doi.org/10.1016/j.jpowsour.2020.228376